THE UNIVERSITY OF

WARWICK

University of Warwick institutional repository: http://go.warwick.ac.uk/wrap

This paper is made available online in accordance with publisher policies. Please scroll down to view the document itself. Please refer to the repository record for this item and our policy information available from the repository home page for further information.

To see the final version of this paper please visit the publisher's website. Access to the published version may require a subscription.

Astronomy
&
Astrophysics

HS 0943+1404, a true intermediate polar[⋆]

P. Rodríguez-Gil[1,2], B. T. Gänsicke[1], H.-J. Hagen[3], D. Nogami[4], M. A. P. Torres[5],
H. Lehto[6,7], A. Aungwerojwit[1], S. Littlefair[8], S. Araujo-Betancor[9], and D. Engels[3]

[1] Department of Physics, University of Warwick, Coventry CV4 7AL, UK
   e-mail: prguez@iac.es
[2] Instituto de Astrofísica de Canarias, Vía Láctea, s/n, La Laguna, 38205 Santa Cruz de Tenerife, Spain
[3] Hamburger Sternwarte, Universität Hamburg, Gojenbergsweg 112, 21029 Hamburg, Germany
[4] Hida Observatory, Kyoto University, Kamitakara, Gifu 506-1314, Japan
[5] Harvard-Smithsonian Center for Astrophysics, 60 Garden St., Cambridge, MA 02138, USA
[6] Tuorla Observatory, Turku University, Väisäläntie 20, 21500 Piikkiö, Finland
[7] Department of Physics, 20014 University of Turku, Finland
[8] School of Physics, University of Exeter, Exeter EX4 4QL, UK
[9] Space Telescope Science Institute, 3700 San Martin Drive, Baltimore, MD 21218, USA

Abstract. We have identified a new intermediate polar, HS 0943+1404, as part of our ongoing search for cataclysmic variables in the Hamburg Quasar Survey. The orbital and white dwarf spin periods determined from time-resolved photometry and spectroscopy are $P_{\mathrm{orb}} \simeq 250$ min and $P_{\mathrm{spin}} = 69.171 \pm 0.001$ min, respectively. The combination of a large ratio $P_{\mathrm{spin}}/P_{\mathrm{orb}} \simeq 0.3$ and a long orbital period is very unusual compared to the other known intermediate polars. The magnetic moment of the white dwarf is estimated to be $\mu_1 \sim 10^{34}$ G cm^3, which is in the typical range of polars. Our extensive photometry shows that HS 0943+1404 enters into deep ($\sim$3 mag) low states, which are also a characteristic feature of polars. We therefore suggest that the system is a true "intermediate" polar that will eventually synchronise, that is, a transitional object between intermediate polars and polars. The optical spectrum of HS 0943+1404 also exhibits a number of unusual emission lines, most noticeably N II λ5680, which is likely to reflect enhanced nitrogen abundances in the envelope of the secondary.

Key words. accretion, accretion disc – stars: binaries: close – stars: novae, cataclysmic variables

1. Introduction

Our understanding of the evolution of cataclysmic variables (CVs) is still very fragmentary. It is clear that the current theory of CV evolution – largely resting on the disrupted magnetic braking scenario (King 1988) – makes a number of predictions in strong conflict with the observational data. For instance, the theoretical minimum orbital period is ~70 min, much shorter than the observed ~80 min (Kolb & Baraffe 1999). In addition, CVs are expected to spend most of their lifetime near the minimum period, a fact not corroborated by the observations.

With regard to the CV populations above and below the period gap, we observe similar numbers of systems on both sides, while all population syntheses predict that ~95% of the entire CV population should have orbital periods below the gap (Kolb 1993; Howell et al. 1997). These three fundamental discrepancies, among others, clearly depict the current misaligning between theory and observations.

Although CV evolution theory has undergone a number of modifications/alternatives (e.g. King & Schenker 2002; Schenker & King 2002; Schenker et al. 2002; Andronov et al. 2003), the discrepancies with the properties of the observed CV population remain unsatisfactorily large, and it seems to be clear that observational selections effects represent a major problem. Gänsicke (2004) has shown that the majority of all CVs have been identified primarily through their variability or through the detection of X-rays, leaving a large parameter space unsampled. We are currently carrying out a large-scale search for CVs based on their spectroscopic properties in the Hamburg Quasar Survey (HQS, Hagen et al. 1995), with the aim of identifying CVs that are inconspicuous in variability or X-ray surveys (Gänsicke et al. 2002b).

[⋆] Based in part on observations obtained at the German-Spanish Astronomical Center, Calar Alto, operated by the Max-Planck-Institut für Astronomie, Heidelberg, jointly with the Spanish National Commission for Astronomy, on observations made with the NOT telescope, operated on the island of La Palma by the Instituto de Astrofísica de Canarias (IAC) at the Spanish Observatorio del Roque de los Muchachos, on observations made with the IAC80 telescope, operated on the island of Tenerife by the IAC at the Spanish Observatorio del Teide, on observations made with the 1.2 m telescope at the FLWO Observatory, a facility of the Smithsonian Institution.

This method proved successful and led to the discovery of a number of systems that show either no or infrequent outbursts, such as e.g. the dwarf nova GY Cnc = HS 0907+1902 (Gänsicke et al. 2000), the SW Sex star HS 0728+6738 (Rodríguez-Gil et al. 2004b), and the enigmatic low-mass transfer system HS 2331+3905 (Araujo-Betancor et al. 2005). Another important class of CVs characterised by rather low levels of variability are those systems containing a magnetic white dwarf, that is rotating either synchronous to the orbital period (polars) or asynchronous (intermediate polars, IPs). The follow-up of HQS CV candidates led to the discovery of a new type of very low mass transfer polars, WX LMi = HS 1023+3900 (Reimers et al. 1999) and HS 0922+1333 (Reimers & Hagen 2000), that may be systems shortly before the onset of Roche-lobe overflow from the secondary; the ultra high-field polar RX J1554.2+2721 = HS 1552+2730 (Jiang et al. 2000; Thorstensen & Fenton 2002; Gänsicke et al. 2004); and the two intermediate polars 1RXS J062518.2+733433 = HS 0618+7336 (Araujo-Betancor et al. 2003) and DW Cnc = HS 0756+1624 (Rodríguez-Gil et al. 2004a).

Here we report on the discovery of the third IP, HS 0943+1404, which exhibits very unusual characteristics, and may be one example of the long-sought link between asynchronous and synchronous magnetic CVs.

2. Observations and data reduction

2.1. Photometry

Differential CCD photometric time series of HS 0943+1404 were obtained during 25 nights throughout the period December 2002 to March 2004, accumulating a total coverage of $\simeq 106$ h (Table 1). The photometric observations were carried out at six different telescopes. Brief details about the individual instrumentation and reduction process are given below.

Calar Alto Observatory. At Calar Alto, filterless and V-band CCD photometry of HS 0943+1404 was obtained in December 2002 and December 2003 with the CAFOS SITe CCD camera on the 2.2 m telescope using a small read-out window. The photometric reduction was carried out using the pipeline described by Gänsicke et al. (2004), which, in brief, pre-processes the images in `ESO-MIDAS` and performs aperture photometry of all stars in the field of view using the `Sextractor` (Bertin & Arnouts 1996). Differential magnitudes of HS 0943+1404 were measured relative to the star "C1" (USNO–A2.0 0975–06331245, $R = 15.9$, $B = 15.9$; see Fig. 1), located $\simeq 30''$ southeast of the CV. The comparison star "C1" was checked against the secondary comparison star "C2" (USNO–A2.0 0975–06331238, $R = 14.3$, $B = 14.6$), and no significant variability was detected. In addition, a number of acquisition images of HS 0943+1404 were obtained prior to spectroscopic observations (Sect. 2.2), at both the 2.2 m and the 3.5 m telescopes, and the magnitude of the target was determined interactively with the `IRAF` task `imexam`, using again the comparison star "C1" in Fig. 1.

Table 1. Log of the photometric observations.

UT Date	Coverage (h)	Filter	Exp. (s)	# Frames	Mean magnitude
Calar Alto 2.2 m					
2001 Apr. 30	–	V	30	1	17.0
2002 Dec. 14	–	V	30	1	17.6
2002 Dec. 15	–	V	30	1	17.6
2002 Dec. 28	1.16	V	45	64	19.2
2003 Mar. 06	–	Clear	20	1	19.1
2003 Dec. 17	1.11	Clear	30	88	16.1
2003 Dec. 23	–	Clear	30	2	16.6
2003 Dec. 23	–	V	30	2	16.5
Calar Alto 3.5 m					
2004 Mar. 02	–	V	30	1	16.7
2004 Mar. 03	–	V	30	1	16.5
FLWO 1.2 m, CCD					
2004 Mar. 09	4.96	Clear	60	407	16.2
2004 Mar. 10	7.70	Clear	60	471	16.3
2004 Mar. 19	3.72	Clear	60	270	16.4
2004 Mar. 20	7.08	Clear	60	605	16.3
IAC80 0.8 m, CCD					
2003 Dec. 27	5.81	Clear	40	500	16.3
2003 Dec. 28	3.19	Clear	40	261	16.4
Tuorla 0.7 m, CCD					
2004 Jan. 20	3.97	Clear	60	217	16.5
2004 Feb. 09	6.89	Clear	60	360	16.4
2004 Mar. 16	5.76	Clear	60	299	16.5
2004 Mar. 18	7.83	Clear	60	395	16.5
Hida 0.6 m, CCD					
2004 Mar. 09	6.64	Clear	60	321	16.4
2004 Mar. 13	2.26	Clear	60	113	16.3
2004 Mar. 15	3.67	Clear	60	191	16.4
2004 Mar. 19	2.67	Clear	60	136	16.4
2004 Mar. 26	0.52	Clear	60	24	16.5
2004 Mar. 27	6.17	Clear	60	296	16.3
2004 Mar. 28	6.60	Clear	60	306	16.4
JKT 1.0 m					
2002 Dec. 29	2.72	Clear	60	120	19.0
2002 Dec. 31	6.25	Clear	60	296	19.0
2003 Jan. 04	2.75	Clear	45	148	18.2
2003 Jan. 05	0.40	Clear	30	32	18.7
2003 Jan. 07	3.52	Clear	45	205	18.9
2003 Jan. 09	2.76	Clear	60	91	19.1

Observatorio del Roque de los Muchachos. On La Palma, filterless CCD photometry of HS 0943+1404 was obtained in December 2002/January 2003 using the Jacobus Kapteyn Telescope (JKT) with the $2 \text{k} \times 2 \text{k}$ pixel^2 SITe detector. Observations and data reduction were carried out in an analogous fashion as described above for the Calar Alto photometry.
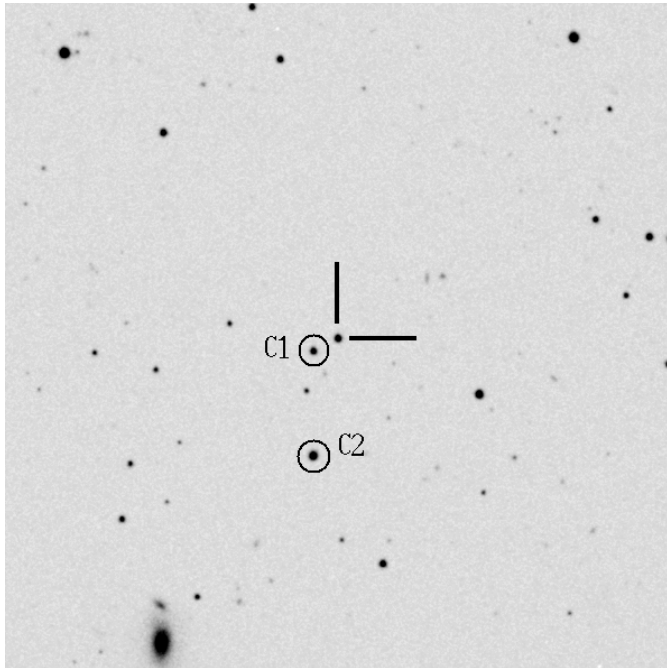
Fig. 1. $10' \times 10'$ finding chart of HS 0943+1404 obtained from the Digitized Sky Survey. The coordinates of the CV are α(J2000) = $09^h46^m34.5^s$, δ(J2000) = $+13°50'58.1''$. North is up and east to the left. "C1" is the primary comparison star and "C2" is the check star.

Fred Lawrence Whipple Observatory. Filterless observations of HS 0943+1404 were carried out with the 1.2 m telescope at the Fred Lawrence Whipple Observatory (FLWO) in March 2004. The 4-Shooter CCD camera was in place, which consists of an array of four 2048×2048 pixel² CCDs. Only a small window of the CCD #3 was read out. Data reduction was carried out using `IRAF`. After bias and flat-field corrections, the images were aligned and instrumental magnitudes of HS 0943+1404 and the comparison stars "C1" and "C2" were extracted using the point spread function (PSF) packages. Differential magnitudes of HS 0943+1404 were then computed relative to "C1".

Observatorio del Teide. Filterless CCD photometry of HS 0943+1404 was obtained at the 0.8 m IAC80 telescope at the Observatorio del Teide on Tenerife in December 2003, using the Thomson 1 k × 1 k pixel² camera. The observations and data reduction were carried out in an analogous way as described above for the FLWO photometry.

Tuorla Observatory. The 0.7 m Schmidt-Vaisala telescope at Tuorla Observatory was used in January, February and March 2004 to obtain filterless photometry of HS 0943+1404 using a SBIG ST–8 CCD camera. Observations and data reduction were carried out in the same way as described above for the Calar Alto photometry.

Hida Observatory. We performed filterless CCD photometry of HS 0943+1404 with the 0.6 m telescope and the SITe CCD camera at Hida Observatory (Japan) in March 2004. After standard reduction of the raw images, differential aperture

Table 2. Log of the spectroscopic observations.

UT Date	Coverage (h)	Grating	Exp. (s)	# Frames
Calar Alto 2.2 m, CAFOS				
2001 Apr. 30	–	B–200	600	1
2002 Dec. 14	0.75	G–100	600	5
2002 Dec. 15	0.76	G–100	600	5
2003 Dec. 23	4.67	G–100	600	22
NOT 2.5 m, ALFOSC				
2003 Dec. 16	4.12	Grism #7	600	24
2003 Dec. 17	6.03	Grism #7	300	64
Calar Alto 3.5 m, MOSCA				
2004 Mar. 01	0.37	G–1000	300	4
2004 Mar. 02	2.08	G–1000	450	15
2004 Mar. 03	3.18	G–1000	450	14

photometry was carried out relative to the comparison star "C1" in a standard manner using `IRAF`.

2.2. Optical spectroscopy

Calar Alto Observatory. An identification spectrum of HS 0943+1404 was obtained on 2001 April 30 at the 2.2 m telescope using the Calar Alto Faint Object Spectrograph (CAFOS) equipped with the standard SITe 2k × 2k pixel² CCD (Table 2). The B–200 grating in conjunction with a 1.5″ slit provided a spectral resolution of ≃10 Å (full width at half maximum, *FWHM*) over the wavelength range $\lambda\lambda 3800-7000$. The spectrum was reduced online using the `MIDAS` quicklook context available at the telescope. The detection of strong Balmer and helium emission lines revealed the likely CV nature of HS 0943+1404.

CAFOS on the 2.2 m telescope was again used in December 2002 and December 2003 to obtain time-resolved, follow-up spectroscopy. The G–100 grism and a slit width of 1.2″ covered the wavelength range $\lambda\lambda 4300-8300$ at a spectral resolution of ≃4.5 Å *FWHM*. The raw images were bias-subtracted and flat-field compensated before removing the sky contribution. The spectra of HS 0943+1404 were optimally extracted according to the algorithm explained in Horne (1986). To achieve a proper wavelength calibration, a low-order polynomial was fitted to the arc data (the rms being less than one tenth of the dispersion in all cases). The pixel-wavelength dependence for each target spectrum was obtained by interpolating between the two nearest arc spectra. The reduction and extraction were performed within `IRAF`[1] and the wavelength calibration was done in `MOLLY`.

Additional time-resolved spectroscopy was carried out in March 2004 using MOSCA on the 3.5 m telescope. The data were obtained with the 2 k × 4 k pixel² SITe CCD camera. The slit width was fixed to 1″ and the G–1000 grism was in place.

---

[1] `IRAF` is distributed by the National Optical Astronomy Observatories.

This setup gave a wavelength range of $\lambda\lambda4200-7400$ at a spectral resolution of $\simeq2.6$ Å (*FWHM*). The data reduction was carried out in the same way as described for the time-resolved CAFOS spectroscopy.

Observatorio del Roque de los Muchachos. The Andalucía Faint Object Spectrograph and Camera (ALFOSC) along with the 2048×2048 pixel[2] EEV chip (CCD #8) were used at the Nordic Optical Telescope (NOT) on La Palma to obtain time-resolved spectroscopy of HS 0943+1404 in December 2003. The combination of grism #7 (plus the second-order blocking filter WG345) and a $1''$ slit provided a resolution of $\simeq3.7$ Å (FHWM) and a useful wavelength range of $\lambda\lambda3800-6800$. As the arc lines projected onto more than 4 pixels (*FWHM*), a 1×2 binning (dispersion direction) was applied. This provided a better signal-to-noise ratio without significantly degrading the spectral resolution. The data reduction was carried out in the same way as explained above.

3. Analysis: photometry

3.1. Long-term variability

From the nightly mean magnitudes presented in Table 1 it is apparent that HS 0943+1404 exhibits pronounced long-term changes in its average brightness. The system was observed at an intermediate magnitude of $V \simeq 17.6$ in mid-December 2002, and in a faint state at $V \simeq 19.0$ from late-December 2002 until March 2003. The transition from the intermediate to the low state hence occured in less than two weeks. By the time of our next observations in December 2003, the system was back to a bright state near $V \simeq 16.3$, where it apparently remained until our last observations in March 2004. Similar long-term variability is observed in strongly magnetic, disc-less CVs (polars) and VY Scl stars (see e.g. Warner 1999). We will hereafter follow the common terminology for these objects, calling the bright state *high state* and the faint state *low state*.

3.2. Short-term variability

In addition to the occurence of high and low states, HS 0943+1404 displays a complex range of short-term variations which we have analysed in detail by computing Scargle periodograms (Scargle 1982) using Schwarzenberg-Czerny's (1989) implementation in the `MIDAS` context `TSA`. After an initial assessment of the periodograms, we have split the photometric data (Table 1) into three separate subsets according to the average brightness of the system, which we discuss below.

3.2.1. December 2002/January 2003 – the low state

The JKT light curves of HS 0943+1404 obtained during the low state show short-term variability superimposed on a low-amplitude modulation (Fig. 2). The Scargle periodogram (Fig. 3, top panel) shows power in three clusters near ~5 d^{-1}, ~15 d^{-1}, and ~22 d^{-1}. The shortness of the individual low-state observations and their poor sampling result in a substantial
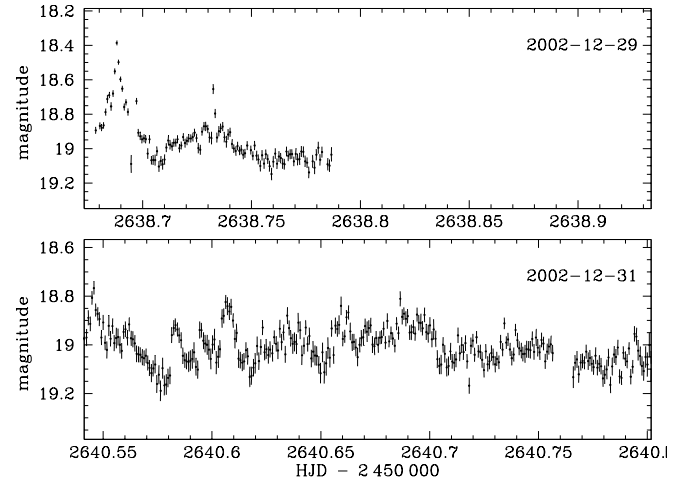

Fig. 2. The low-state photometry obtained with the JKT in December 2002/January 2003 shows evidence of short-lived flares (*top*), and a low-amplitude, long-period (several hours) modulation superimposed on short-period variability.
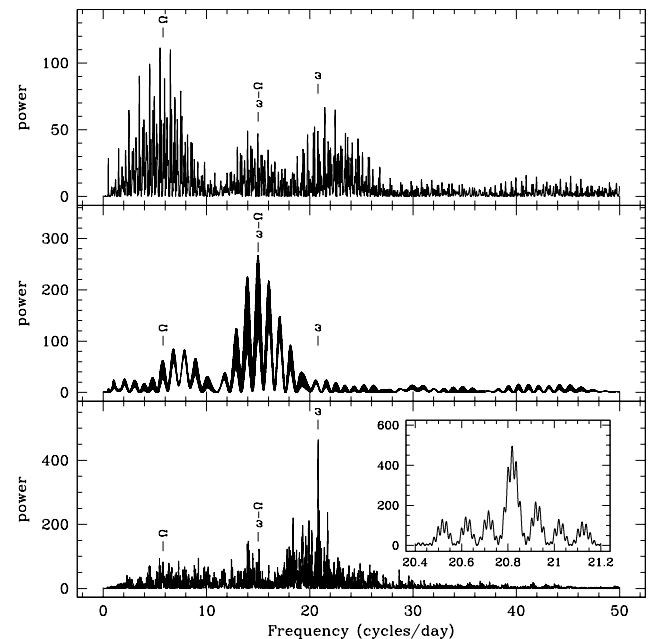

Fig. 3. Scargle periodograms computed from three subsets of the CCD photometry listed in Table 1. *Top panel*: periodogram for the low state data obtained in December 2002/January 2003. Three clusters of signals are evident at ~5 d^{-1}, ~15 d^{-1}, and ~22 d^{-1}. *Middle panel*: periodogram of the December 2003 IAC80 data and the February 2004 Tuorla data. The dominant signal is found at 15 d^{-1} (plus one-day aliases), and a weaker signal at 6.8 d^{-1} (plus one-day aliases). *Bottom panel*: periodogram for the January 2004 Tuorla data and the March 2004 campaign. The strongest signal is detected at 20.8 d^{-1}, a second cluster of signals is present near 15 d^{-1}. The inset shows a close-up of the 20.8 d^{-1} signal. We identify the 20.8 d^{-1} frequency with the white dwarf spin ω ($P_{\text{spin}} = 69.2$ min), and the 15 d^{-1} frequency with the beat between the white dwarf spin and the orbital motion $\omega-\Omega$, which implies an orbital frequency of $\Omega = 5.8$ d^{-1} ($P_{\text{orb}} = 248$ min).

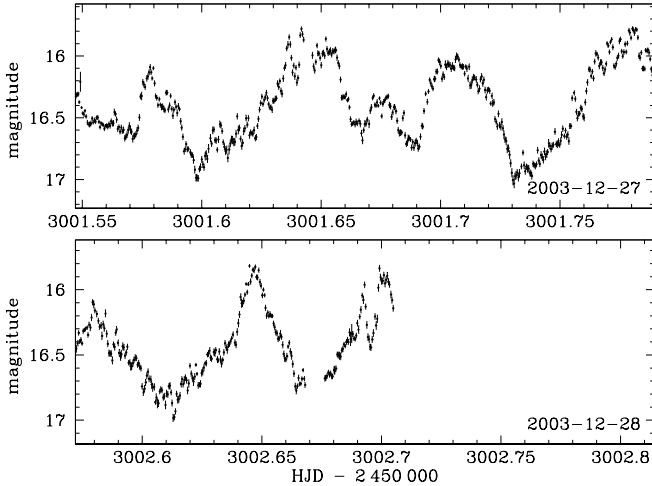number of aliases in all three ranges, impeding a more detailed analysis.

Fig. 4. During the two nights of IAC80 observations, HS 0943+1404 displayed a photometric variability with a period of $\simeq$96 min, which we interpret as the beat period.

Fig. 5. Sample light curves obtained at FWLO, Hida Observatory, and Tuorla observatory during the March 2004 campaign. The data show a periodic modulation with a period of $\simeq$69 min, which we identify with the white dwarf spin period.

3.2.2. December 2003 & February 2004 – a 96 min modulation in high state

The light curves obtained during the December 2003 IAC80 (Fig. 4) and the February 2004 Tuorla runs display a large-amplitude ($\simeq$0.5 mag) modulation with a period of $\simeq$96 min. The Scargle periodogram of these three nights of data (Fig. 3, middle panel) confirms this visual estimate, being dominated by a signal at $15\,\mathrm{d}^{-1}$ (plus one-day aliases thereof). A second weaker signal is found at $6.8\,\mathrm{d}^{-1}$, also flanked by one-day aliases. Variability on shorter time scales than the dominant 96-min modulation is seen in the light curves, but the periodogram contains no strong signal at higher frequencies.

3.2.3. January & March 2004 campaign – a 69 min modulation in high state

The light curves obtained in January 2004 at the Tuorla Observatory and during the March 2004 multi-site campaign carried out at FLWO, Hida Observatory, and Tuorla Observatory are dominated by a coherent signal with a period of $\simeq$69 min and an amplitude of 0.2–0.3 mag (Fig. 5). The Scargle periodogram of this data set (Fig. 3, bottom panel) is dominated by a sharp signal at $20.8\,\mathrm{d}^{-1}$, and contains some weaker signals in the range 14–$15.2\,\mathrm{d}^{-1}$.

3.3. An intermediate polar interpretation

Complex short-term variability characterized by the presence of several coherent signals is the hallmark of IPs, CVs containing a moderately magnetic white dwarf with a spin period shorter than the orbital period, $P_{\mathrm{spin}} < P_{\mathrm{orb}}$. The power spectra of IPs typically show signals at the orbital frequency Ω, the white dwarf spin frequency ω, and the beat (i.e. synodic) frequency $\omega - \Omega$ (additional beat signals at $\omega + \Omega$ or $\omega - 2\Omega$ have been detected in some IPs, e.g. Warner 1986).

Considering the morphology of the observed light curves and the resulting periodograms, we suggest that HS 0943+1404
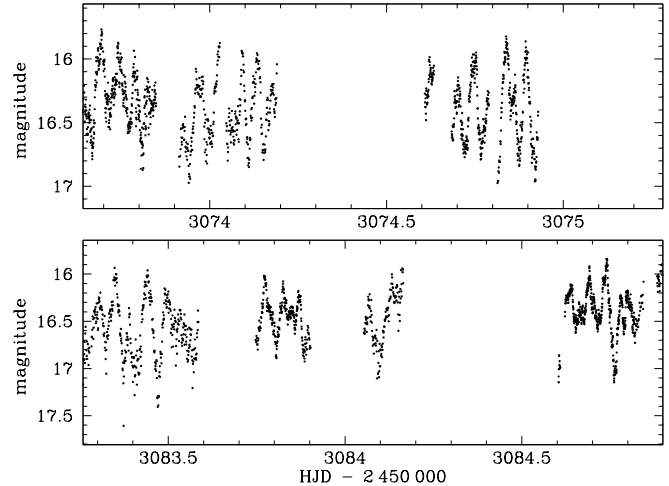
is an IP. We identify the highly coherent, highest frequency signal detected in the photometry of HS 0943+1404 with the white dwarf spin, the intermediate frequency signal as the beat between white dwarf spin and orbital periods, and the lowest frequency signal with the orbital period. The spin signal in the bottom panel of Fig. 3 shows some alias substructure due to the long gap between the January 2004 and March 2004 data. The frequency of the central peak is $20.8179 \pm 0.0003\,\mathrm{d}^{-1}$, with the two flanking aliases located at $20.8011 \pm 0.0003\,\mathrm{d}^{-1}$ and $20.8348 \pm 0.0003\,\mathrm{d}^{-1}$, where the errors given in brackets have been determined by fitting a sine wave to the data. The beat signal (Fig. 3, middle panel) is also plagued by multiple aliases due to the separation of the December 2003 and February 2004 runs. The strongest signal is found at $15.0 \pm 0.2\,\mathrm{d}^{-1}$, where the error in brackets is conservatively estimated from half the *FWHM* of the central cluster of aliases.

We conclude that HS 0943+1404 is an IP, and the analysis of our photometric data results in $P_{\mathrm{spin}} = 69.171 \pm 0.001$ min, $P_{\mathrm{beat}} = 96.0 \pm 3.3$ min, and $P_{\mathrm{orb}} = 247.5 \pm 3.3$ min. Figure 6 shows the spin and beat-dominated data folded on the spin and beat period, respectively.

4. Analysis: spectroscopy

4.1. The optical spectrum of HS 0943+1404

The spectrum of HS 0943+1404 (Fig. 7) is dominated by strong, single-peaked emission lines of H I and He I. He II line emission at $\lambda\lambda 4686,5412$, and the Bowen blend are also prominent, indicating the presence of a source of high-energy photons. The relative strength of these emission lines is reminiscent of the magnetic CVs. The continuum significantly rises bluewards of Hα and atmospheric features of the secondary star are absent in the observed spectral ranges.

The most remarkable feature in the optical spectrum of HS 0943+1404 is the strength of several emission lines that are either very weak or absent in most other CVs, such as Fe II
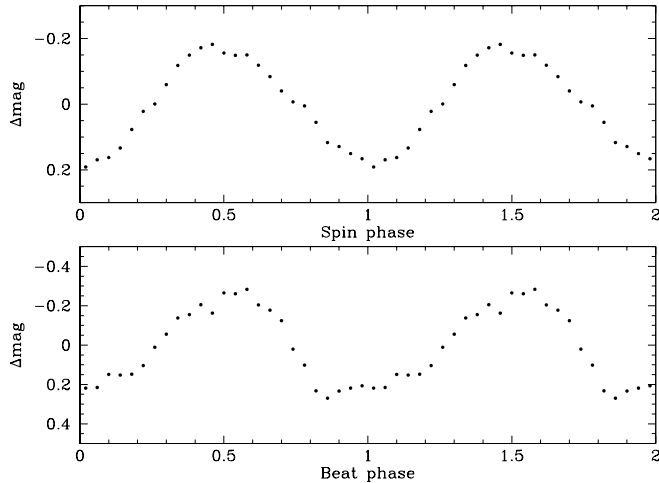
Fig. 6. *Top panel*: the January 2004 and March 2004 data folded on the white dwarf spin period of 69.2 min. *Bottom panel*: the December 2003 and February 2004 data folded on the beat period of 96 min.
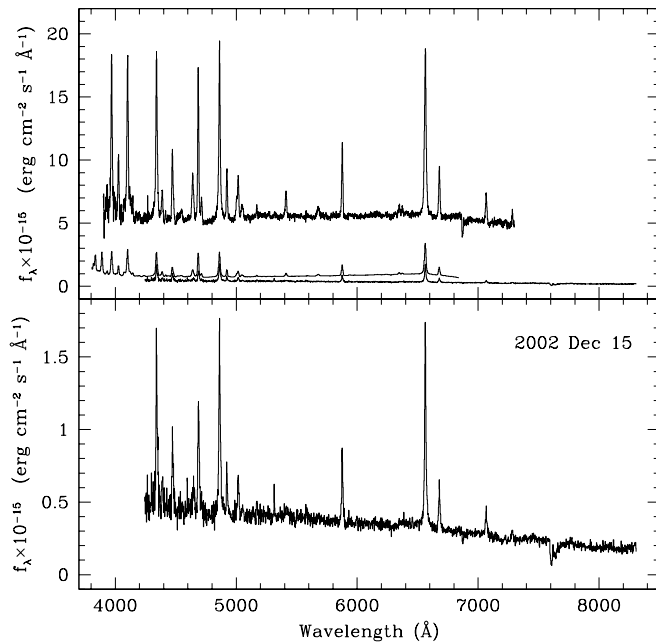

Fig. 7. *Top panel*: flux calibrated average spectra of HS 0943+1404 taken in different epochs. From *bottom* to *top*, 2002 December 15 (Calar Alto 2.2 m), 2003 December 16–17 (NOT), and 2004 March 1–3 (Calar Alto 3.5 m). These spectra nicely illustrate the rather frequent brightness changes of HS 0943+0414. *Bottom panel*: enlarged version of the lower spectrum shown in the top panel (2002 December). The system was in an intermediate state near $V = 17.6$ mag. No spectroscopic signature of the donor star is evident in the red part of the spectrum.

(e.g. $\lambda5018$, 5169), N II $\lambda5680$, Si II $\lambda6347,6372$, and probably Al II $\lambda6243$ (see the $\lambda\lambda4900$–6500 range of the 2003 December NOT average spectrum; Fig. 8). A closer inspection reveals that the spectrum of HS 0943+1404 shows abundant weak emission lines throughout. In Table 3 we present the equivalent widths (*EW*s) of the most prominent lines as measured in the average spectra corresponding to the three different epochs.
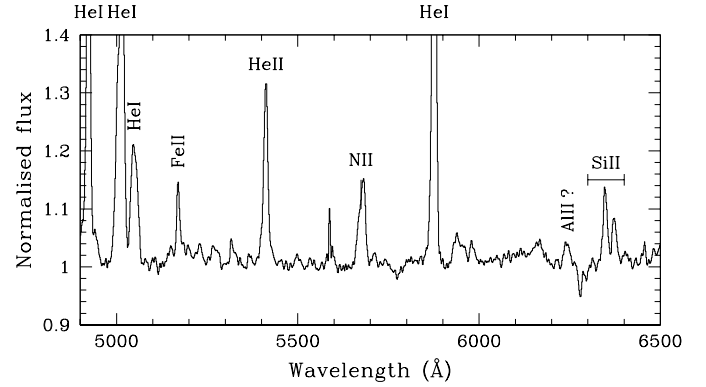

Fig. 8. Average spectrum of HS 0943+1404 (2003 December, NOT) showing a number of unusual emission lines in the range $\lambda\lambda4900$–6500. Note the strong N II $\lambda5680$ and Si II $\lambda6347$ and $\lambda6371$.

Table 3. Line equivalent widths measured from the average spectra.

Line	EW (Å)	Line	EW (Å)
2002 December (intermediate state)			
Hα	70	He I $\lambda6678$	13
Hβ	48	He I $\lambda5876$	18
Hγ	33	He I $\lambda4922$	7
He II $\lambda4686$	25	He I $\lambda4472$	11
He II $\lambda5412$	4	He I $\lambda4388$	3
Bowen blend	6	N II $\lambda5680$	2
He I $\lambda7065$	10		
2003 December (high state)			
Hα	53	He I $\lambda7281$	5
Hβ	49	He I $\lambda7065$	9
Hγ	44	He I $\lambda6678$	12
Hδ	42	He I $\lambda5876$	16
Hε	32	He I $\lambda4922$	10
H8	22	He I $\lambda4472$	16
H9	13	He I $\lambda4388$	7
He II $\lambda4686$	35	He I $\lambda4026$	11
He II $\lambda5412$	6	N II $\lambda5680$	4
Bowen blend	16		
2004 March (high state)			
Hα	52	He I $\lambda6678$	13
Hβ	51	He I $\lambda5876$	14
He II $\lambda4686$	31	He I $\lambda4922$	10
He II $\lambda5412$	8	He I $\lambda4472$	19
Bowen blend	17	He I $\lambda4388$	9
He I $\lambda7065$	9	N II $\lambda5680$	5

4.2. Radial velocity variations

In order to search for orbital variability, we measured the radial velocities of the Hα, Hβ, He I $\lambda5876$ and He II $\lambda4686$ emission lines. The spectra were first re-binned to a constant velocity scale centred at the rest wavelength of each line and normalised. Radial velocities were measured by using three different methods: (i) correlation with a single Gaussian template; (ii) the double Gaussian technique of Schneider & Young (1980); and (iii) calculation of the median velocity (the point leaving the same area on both sides of the normalised line
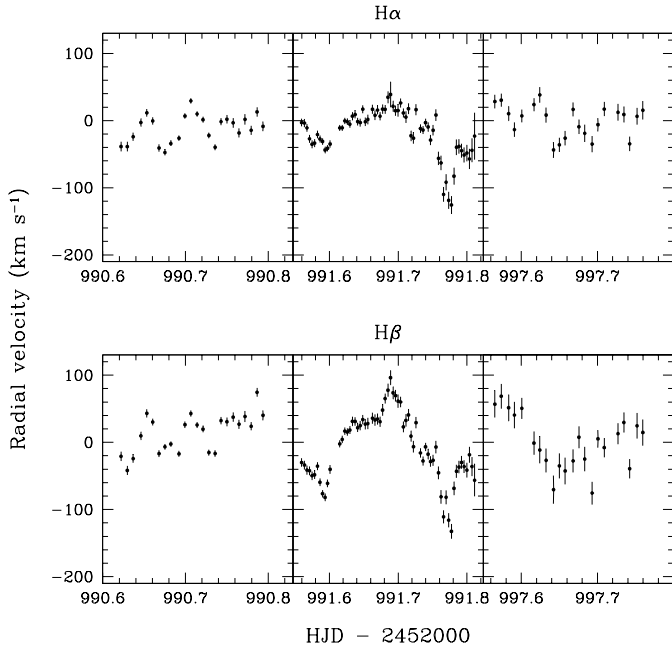
Fig. 9. Hα (*top*) and Hβ (*bottom*) radial velocity curves. From *left* to *right*: 2003 December 16, 17, and 23.

profile). The latter method proved to be the most efficient, producing the cleanest radial velocity curves. The resulting curves for Hα and Hβ are shown in Fig. 9.

The morphology of the radial velocity curves seems to significantly change from night to night. On 2003 December 16, a modulation at ∼70 min dominates, whereas a longer time scale modulation is clearly seen on 2003 December 17. On this night, a dip towards blue velocities at HJD ≃ 2 452 991.77 is observed. A shallower excursion to the blue also occurs at HJD ≃ 2 452 991.59. The separation between them was measured by fitting Gaussians to the dips, obtaining a value of ≃0.19 d. In addition, the Hβ curve displays a red spike centred at ≃2452991.69, almost just in the middle of the blue dips. A sine fit to the Hβ radial velocity curve (after masking the dips) yields a period of ≃0.19 d and a semi-amplitude of ∼45 km s^{-1}.

In order to search for periodicities we computed Scargle periodograms (Scargle 1982) for all the Hα, Hβ, He I λ5876, and He II λ4686 radial velocity curves. The periodograms for all the lines are very similar, and we present in Fig. 10 only the periodograms for Hβ and He II λ4686. Both periodograms are dominated by clusters of aliases near ≃3.4, 4.4, and 5.4 d^{-1}. The poor sampling of our radial velocities spread out over 15 months causes severe fine-structure in the main alias clusters, and impedes an unequivocal identification of the frequency inherent to the system. Formally, the strongest signal in the Hβ radial velocity variation is found at 5.430 ± 0.002 d^{-1} (the quoted error is a conservative estimate from the width of the peak in the periodogram), which corresponds to a period of P = 0.18416 ± 0.00007 d (= 265.2 ± 0.1 min). In the case of He II λ4686, a value of 4.412 ± 0.005 d^{-1} (P = 0.2267 ± 0.0003 d = 325.8 ± 0.4 min) is found. The presence of power around 250 min in both the low-state photometry (Fig. 3, top panel) and in the radial velocity variations (Fig. 10) strongly suggests the detection of a "clock" in HS 0943+1404.
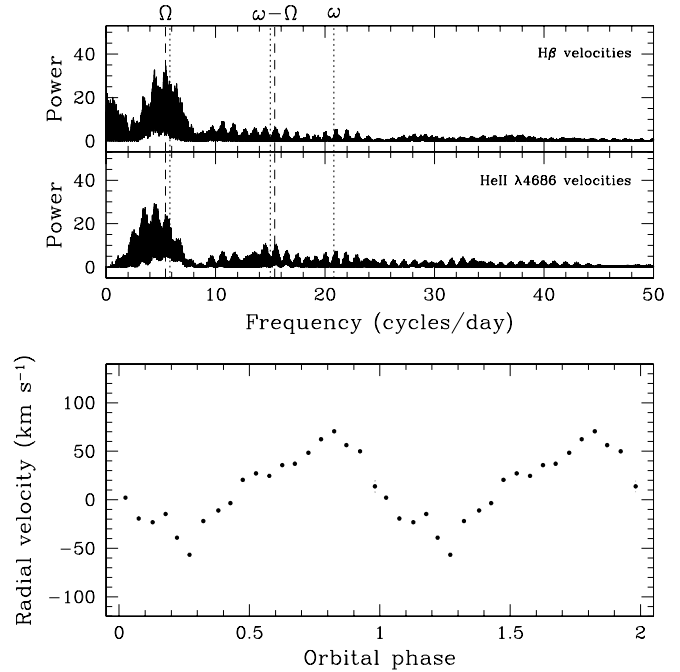

Fig. 10. *Top*: scargle periodograms of the Hβ and He II λ4686 radial velocity curves. Ω is the orbital frequency, ω the white dwarf spin, and ω − Ω the corresponding synodic frequency. Dashed (dotted) vertical lines correspond to spectroscopic (photometric) results. *Bottom*: Hβ radial velocity curve folded on 265.2 min after averaging the data into 20 phase bins. The time of red-to-blue crossing is T_0 = 2 452 623.78160 (HJD). The orbital cycle has been plotted twice for continuity.

Given that this is the longest period detected in all our data we believe that it represents the orbital motion of the binary.

The Hβ radial velocities folded on 265.2 min, the strongest signal in the Hβ periodogram, displays a relatively low-amplitude modulation superimposed by a short (∼0.15 orbital phase) negative excursion, which is mostly related to the two "dips" seen in the December 17 NOT data.

4.3. V/R ratios and equivalent width curves

Our second approach at searching for periodicities involved the analysis of the Hα, Hβ, He I λ5876 and He II λ4686 V/R-ratio and EW curves. The V/R ratio is computed by dividing the EW of the blue half of the line profile (up to zero velocity, i.e. the V part) by that of the red half (redwards from zero velocity; the R part). Only the Scargle periodograms for Hβ and He II λ4686 are shown in Fig. 11. The picture in the low frequency regime does not shed new light on the orbital period discussion, as it contains the same three clusters of aliases around 3.4, 4.4, and 5.4 d^{-1}. However, the EW periodograms contain a strong peak at the photometric spin frequency. The strongest peak in both the Hβ and He II λ4686 EW periodograms is centred at 20.82 d^{-1}, exactly at the spin frequency.
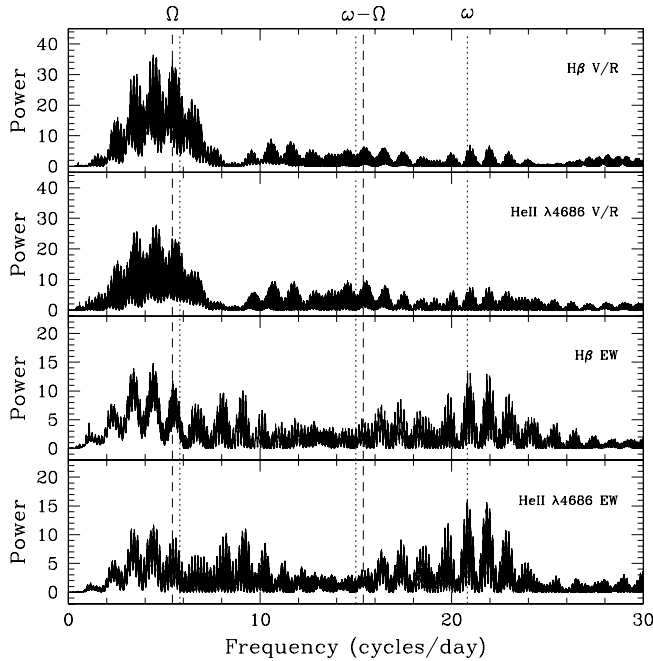
Fig. 11. Scargle periodograms of the Hβ and He II λ4686 *V/R* and *EW* curves. Dashed (dotted) vertical lines correspond to spectroscopic (photometric) results.

5. Discussion

5.1. The intermediate polar nature of HS 0943+1404

The combined photometric and spectroscopic results clearly qualify HS 0943+1404 as an asynchronous magnetic CV, an IP. The system has a likely orbital period of $P_{\rm orb} \simeq 250$ min and a white dwarf spin period of $P_{\rm spin} = 69.171 \pm 0.001$ s. The radial velocity analysis of our spectroscopy suggests $P_{\rm orb} = 265.2$ min, while the more extensive photometry suggests $P_{\rm orb} = 247.5$ min from the detection of the beat and spin periods.

The combination of orbital and spin periods found in HS 0943+1404 is rather unusual, as it yields a large $P_{\rm spin}/P_{\rm orb} \simeq 0.3$ and a long orbital period. The only other known IPs with even larger $P_{\rm spin}/P_{\rm orb}$ are EX Hya (Vogt et al. 1980), V1025 Cen (Buckley et al. 1998), and DW Cnc (Rodríguez-Gil et al. 2004a), all three are short-period systems below the period gap. The majority of IPs are concentrated near $P_{\rm spin}/P_{\rm orb} \simeq 0.1$ (see e.g. Barrett et al. 1988; King & Lasota 1991; Warner & Wickramasinghe 1991), but King & Wynn (1999) showed that spin-orbit equilibria exist with $P_{\rm spin}/P_{\rm orb} > 0.1$, explaining cases such as EX Hya. Most recently, Norton et al. (2004) demonstrated that a large range of permitted spin-orbit equilibria exists in the ($P_{\rm spin}/P_{\rm orb}, \mu_1$) parameter space, with μ_1 the magnetic moment of the white dwarf primary star. We used their Fig. 2 to estimate a magnetic moment of $\mu_1 \sim 10^{34}$ G cm^3 for HS 0943+1404. This value is in the typical range found for polars, and assuming an average white dwarf ($M_{\rm wd} \simeq 0.65\,M_\odot$, $R_{\rm wd} \simeq 10^8$ cm) would result in a magnetic dipole field strength of ~20 MG. Hence, it appears entirely possible that HS 0943+1404 is a true "intermediate" polar, that will synchronise once its orbital period and mass

transfer rate decrease sufficiently – in fact, for the parameters determined here, HS 0943+1404 lies above the synchronisation line in Fig. 4 of Norton et al. (2004).

Another property that HS 0943+1404 shares with polars is the occurence of deep ($\simeq 3$ mag) low states, such as the one observed in January 2003 (Table 1). Such low states are characteristic of polars, only one long-period IP is known to have entered a deep low state (see e.g. Warner 1999).

5.2. Spin-beat period switching

Our photometric data show that HS 0943+1404 switches between states which are either dominated by variability at the white dwarf spin period, or by variability at the beat period. Changes in the relative power of the spin signal with respect to the side-band signals have been observed in other IPs, such as TX Col (Buckley & Tuohy 1989; Norton et al. 1997), and in V1062 Tau, where at a given time only the spin or the beat period is detected (Lipkin et al. 2004). In V1062 Tau, Lipkin et al. (2004) suggested that the switching between spin- and beat-dominated variability is triggered by changes in the system brightness which they relate to changes in the mass transfer rate.

A dominating signal at the beat period has been interpreted as a sign of disc-less accretion (e.g. Buckley et al. 1995; Hellier 2002, and references therein). Spin-dominated variability is generally explained by disc-fed accretion. The variations are thought to arise from reprocessing of X-rays at either the inner edge or the outer rim of the magnetically-truncated disc (Warner 1986), or from aspect variations of the accretion funnel feeding material from the inner disc edge onto the white dwarf (see e.g. Hellier et al. 1987).

The alternating dominance of the spin and beat signals in the light curves of HS 0943+1404 clearly implies changes in the accretion mode. However, in this system, both states have been observed at similar mean brightness levels (Table 1, Figs. 4 and 5). The fact that the spectrum of the secondary star is not detected even when the system is faint (although no spectrum in low state is available; see Fig. 7) indicates that the accretion disc must dominate the observed continuum. Hence, a predominant signal at the beat period cannot be unambiguously linked to disc-less accretion. All of this suggests that changes in the accretion mode are not solely due to variations in the mass transfer rate, but can also be triggered by other mechanisms within the binary system (Norton et al. 1997).

5.3. An elevated nitrogen abundance

The optical spectrum of HS 0943+1404 is similar to that of the IP 1RXS J062518.2+733433 (=HS 0618+7336; Araujo-Betancor et al. 2003). Both systems show unusually strong emission of N II λ5680 compared to most other CVs. We interpret this as evidence for an enhanced nitrogen abundance in these two IPs, which is usually associated with the existence of CNO-processed material in the envelope of the donor star. Two possible scenarios can explain the origin of the CNO-processed material in the envelope of the donor: either the

companion has accreted material from the shell associated with a nova explosion on the white dwarf, or the secondary star is evolved (and the white dwarf is accreting material from the exposed CNO core whose outer layers were stripped off during a thermal time-scale mass-transfer phase, see Schenker et al. 2002; Podsiadlowski et al. 2003). Based on a HST FUV survey of cataclysmic variables, Gänsicke et al. (2003) have recently shown that 10%–15% of all CVs display enhanced nitrogen abundances. This is in agreement with the predictions by Schenker et al. (2002) and Podsiadlowski et al. (2003) that a non-negligible fraction of all CVs should have evolved through a phase of thermal time scale mass transfer.

6. Conclusions

The results presented in this paper are summarised as follows:

1. Based on our photometric and spectroscopic observations, we have shown that HS 0943+1404 is a new intermediate polar CV with an orbital period of $P_{orb} \simeq 250$ min and a white dwarf spin period of $P_{spin} = 69.171 \pm 0.001$ s. An additional confirmation of the spin period, e.g. through the detection of a coherent variablity in X-rays or polarised light would be desirable.

2. Based on Norton et al.'s (2004) calculations, we estimate the magnetic moment of the white dwarf in HS 0943+1404 to be $\mu_1 \sim 10^{34}$ G cm^3, which is in the range of polars. Long-term photometric monitoring of the system revealed the occurrence of deep low states, during which the brightness drops by ~3 mag, also typical of polars. It appears likely that HS 0943+1404 is a true "intermediate" polar on its way to synchronization.

3. The optical spectrum of HS 0943+1404 contains a number of unusual emission lines, most noticeably N II $\lambda 5680$, which suggests the presence of CNO-enriched material in the envelope of the secondary star. Ultraviolet spectroscopy of HS 0943+1404 would be useful to assess the carbon and nitrogen abundances from the N V $\lambda 1240$ and C IV $\lambda 1550$ resonance lines.

References

Andronov, N., Pinsonneault, M., & Sills, A. 2003, ApJ, 582, 358
Araujo-Betancor, S., Gänsicke, B. T., Hagen, H.-J., et al. 2005, A&A, 430, 629
Araujo-Betancor, S., Gänsicke, B. T., Hagen, H.-J., Rodríguez-Gil, P., & Engels, D. 2003, A&A, 406, 213
Barrett, P., O'Donoghue, D., & Warner, B. 1988, MNRAS, 233, 759
Bertin, E., & Arnouts, S. 1996, A&AS, 117, 393

Buckley, D. A. H., Cropper, M., Ramsay, G., & Wickramasinghe, D. T. 1998, MNRAS, 299, 83
Buckley, D. A. H., Sekiguchi, K., Motch, C., et al. 1995, MNRAS, 275, 1028
Buckley, D. A. H., & Tuohy, I. R. 1989, ApJ, 344, 376
Gänsicke, B. T. 2004, in Compact Binaries in the Galaxy and Beyond, ed. G. Tovmassian, & E. Sion, Conf. Ser. 20, Rev. Mex. Astron. Astrofís., 152
Gänsicke, B. T., Araujo-Betancor, S., Hagen, H.-J., et al. 2004, A&A, 418, 265
Gänsicke, B. T., Szkody, P., de Martino, D., et al. 2003, ApJ, 594, 443
Gänsicke, B. T., Fried, R. E., Hagen, H.-J., et al. 2000, A&A, 356, L79
Gänsicke, B. T., Beuermann, K., & Reinsch, K., ed. 2002a, The Physics of Cataclysmic Variables and Related Objects, ASP Conf. Ser., 261
Gänsicke, B. T., Hagen, H. J., & Engels, D. 2002b, in The Physics of Cataclysmic Variables and Related Objects, ed. B. T. Gänsicke, K. Beuermann, & K. Reinsch, ASP Conf. Ser., 261, 190
Hagen, H. J., Groote, D., Engels, D., & Reimers, D. 1995, A&AS, 111, 195
Hellier, C. 2002, in The Physics of Cataclysmic Variables and Related Objects, ed. B. T. Gänsicke, K. Beuermann, & K. Reinsch, ASP Conf. Ser., 261, 92
Hellier, C., Mason, K. O., Rosen, S. R., & Cordova, F. A. 1987, MNRAS, 228, 463
Horne, K. 1986, PASP, 98, 609
Howell, S. B., Rappaport, S., & Politano, M. 1997, MNRAS, 287, 929
Jiang, X. J., Engels, D., Wei, J. Y., Tesch, F., & Hu, J. Y. 2000, A&A, 362, 263
King, A. R. 1988, QJRAS, 29, 1
King, A. R., & Lasota, J. P. 1991, ApJ, 378, 674
King, A. R., & Schenker, K. 2002, in The Physics of Cataclysmic Variables and Related Objects, ed. B. T. Gänsicke, K. Beuermann, & K. Reinsch, ASP Conf. Ser., 261, 233
King, A. R., & Wynn, G. A. 1999, MNRAS, 310, 203
Kolb, U. 1993, A&A, 271, 149
Kolb, U., & Baraffe, I. 1999, MNRAS, 309, 1034
Lipkin, Y. M., Leibowitz, E. M., & Orio, M. 2004, MNRAS, 349, 1323
Norton, A. J., Hellier, C., Beardmore, A. P., et al. 1997, MNRAS, 289, 362
Norton, A. J., Wynn, G. A., & Somerscales, R. V. 2004, ApJ, 614, 349
Podsiadlowski, P., Han, Z., & Rappaport, S. 2003, MNRAS, 340, 1214
Reimers, D., & Hagen, H. J. 2000, A&A, 358, L45
Reimers, D., Hagen, H. J., & Hopp, U. 1999, A&A, 343, 157
Rodríguez-Gil, P., Gänsicke, B. T., Araujo-Betancor, S., & Casares, J. 2004a, MNRAS, 349, 367
Rodríguez-Gil, P., Gänsicke, B. T., Barwig, H., Hagen, H.-J., & Engels, D. 2004b, A&A, 424, 647
Scargle, J. D. 1982, ApJ, 263, 835
Schenker, K., & King, A. R. 2002, in The Physics of Cataclysmic Variables and Related Objects, ed. B. T. Gänsicke, K. Beuermann, & K. Reinsch, ASP Conf. Ser., 261, 242
Schenker, K., King, A. R., Kolb, U., Wynn, G. A., & Zhang, Z. 2002, MNRAS, 337, 1105
Schneider, D. P., & Young, P. 1980, ApJ, 238, 946
Schwarzenberg-Czerny, A. 1989, MNRAS, 241, 153
Thorstensen, J. R., & Fenton, W. H. 2002, PASP, 114, 74
Vogt, N., Krzeminski, W., & Sterken, C. 1980, A&A, 85, 106
Warner, B. 1986, MNRAS, 219, 347
Warner, B. 1999, in Annapolis Workshop on Magnetic Cataclysmic Variables, ed. C. Hellier, & K. Mukai, ASP Conf. Ser., 157, 63
Warner, B., & Wickramasinghe, D. T. 1991, MNRAS, 248, 370